buildings

MDPI

Article

Local Climate Zone in Xi'an City: A Novel Classification Approach Employing Spatial Indicators and Supervised Classification

Duo Xu [1], Qian Zhang [2,*], Dian Zhou [1,*], Yujun Yang [1], Yiquan Wang [1] and Alessandro Rogora [2]

[1] School of Human Settlements and Civil Engineering, Xi'an Jiaotong University, Xi'an 710049, China; duo_xu@xjtu.edu.cn (D.X.); yujun_yang@mail.xjtu.edu.cn (Y.Y.); wang_yq@stu.xjtu.edu.cn (Y.W.)
[2] Department of Architecture and Urban Studies, Politecnico di Milano, 20156 Milan, Italy; alessandro.rogora@polimi.it
* Correspondence: qian.zhang@polimi.it (Q.Z.); dian-z@mail.xjtu.edu.cn (D.Z.)

Abstract: The Local Climate Zone (LCZ), as a foundational element of urban climate zone classification proposed by Oke and Stewart, categorizes urban surface types based on 10 influential parameters affecting the urban heat island effect, such as building density, surface reflectivity, sky view factor, and surface roughness length. This method divides cities into 17 different Local Climate Zones (LCZs) to standardize climate observations and promote global climate research exchange, offering valuable insights for heat island studies. In this study, we enhance the existing local climate zones spatial classification approach by focusing on Xi'an city's urban layout and architectural features. By using urban spatial indicators and employing a supervised classification approach and a spatial clustering method with land parcels as statistical units, we investigate typical urban areas and classify Xi'an's land parcels into 17 or 15 distinct local climate zones. Subsequently, through the evaluation of two distinct classification methods, the most suitable urban microclimate zoning method for Xi'an city was selected. This optimization of the local climate zoning representation introduces a spatial classification method tailored to urban climate planning and control, utilizing urban spatial indicators and remote sensing data. The resulting urban climate zoning map not only supports sample selection for urban heat environment parameter observation but also aids urban planners in identifying spatial distribution patterns for climate zoning.

Keywords: local climate zone; urban heat island; multi-source data; supervised spatial classification

check for updates

Citation: Xu, D.; Zhang, Q.; Zhou, D.; Yang, Y.; Wang, Y.; Rogora, A. Local Climate Zone in Xi'an City: A Novel Classification Approach Employing Spatial Indicators and Supervised Classification. *Buildings* **2023**, *13*, 2806. https://doi.org/10.3390/buildings13112806

Academic Editor: Adrian Pitts

Received: 18 October 2023
Revised: 2 November 2023
Accepted: 7 November 2023
Published: 9 November 2023

Copyright: © 2023 by the authors. Licensee MDPI, Basel, Switzerland. This article is an open access article distributed under the terms and conditions of the Creative Commons Attribution (CC BY) license (https://creativecommons.org/licenses/by/4.0/).

1. Introduction

Urban climates exhibit intricate spatial and temporal variations, necessitating a comprehensive understanding of urban heat environments for effective urban planning and climate investigations. Local Climate Zones (LCZs) have emerged as a prominent classification system for urban climate analysis, offering a comprehensive framework to delineate climate characteristics and their associated spatial attributes [1]. Initially introduced by Oke and Stewart as an extension of the Urban Climate Zone (UCZ) classification, the LCZ classifies urban areas into 17 distinct local climate zones based on parameters that influence the urban heat island effect. These parameters include building density, surface reflectance, sky view factor, and surface roughness length [2]. The primary objective of the LCZ framework is to standardize climate observations and facilitate global exchange in climate research [3].

The LCZ classification system has paved the way for innovative research into urban heat islands, offering practical applications in the layout of urban weather stations, the assessment of outdoor comfort [4], the standardization of urban weather condition reporting, and the comparative analysis of heat island effects across different cities [5,6]. The LCZ

classification system also offers an objective measure of the heat island intensity, prompting investigations into the causative factors underlying the urban heat island effect [6].

At present, the LCZ systems are a burgeoning focal point at the intersection of meteorology and urban planning, representing a relatively recent development in the field of urban climate studies. Three primary methodologies are employed for the LCZ classification: manual supervised classification, remote sensing image recognition, and classification based on ArcGIS urban spatial databases [7]. Manual classification, although thorough, is time-consuming and lacks standardization, limiting its practicality for widespread adoption. In recent years, remote sensing techniques have gained prominence due to their ability to expedite and standardize the classification process, utilizing machine learning algorithms to categorize pixels based on the spectral characteristics of urban satellite imagery. However, this approach may yield reduced accuracy and fragmented outcomes in densely populated cities like Hong Kong, raising concerns about its suitability for classifying high-density Chinese urban areas.

Conversely, the ArcGIS urban spatial database classification method necessitates more extensive urban spatial and planning data, involves more computational effort, and consumes more time. Nonetheless, this approach enhances the quantification of urban spatial information, augmenting data accuracy and enabling the precise identification of various surface types within urban regions. Moreover, it affords the flexibility to tailor classification criteria to the unique characteristics of each city, rendering it suitable for urban climate planning and integration with a city's development control system.

In China, the application of the LCZ system in urban climate research is still in its nascent stages, with only a limited number of studies conducted in major cities. For instance, Chen Fangli and colleagues employed the World Urban Database and Access Portal Tools (WUDAPT) database to construct a LCZ map for Chengdu's central urban area and explored the utility of a LCZ in urban planning [8]. Meng Cai and his team established a quantitative link between urban surface temperature and local climate zones, devising an improved method within WUDAPT to generate the LCZ maps for the extensive Yangtze River Delta region in China. Their findings revealed that distinct urban LCZ classifications corresponded to elevated land surface temperatures [9]. Xiaoshan Yang and his collaborators conducted temperature measurements across various LCZ areas in Nanjing to evaluate the thermal behavior of different local climate zones. They quantitatively analyzed the thermal characteristics of different LCZ types, showcasing how each LCZ type exhibited thermal behavior associated with its surface structure and land cover attributes, thereby underscoring the utility of the LCZ in comprehensive climate-oriented classification systems [10].

The evolving field of LCZ research presents an opportunity for China to deepen its understanding of urban climates and inform urban planning in the context of rapid urbanization. This study aims to contribute to the expanding body of LCZ research by examining the applicability and ramifications of the LCZ classification in Chinese cities, with a particular focus on high-density urban areas. Through this research, we endeavor to address the following objectives and broaden our comprehension of LCZ's potential in urban climate studies and planning.

1.1. Impact of Urbanization on Urban Climate

In developing nations, the rapid expansion of urban areas has induced profound alterations in Land Use/Land Cover (LULC), urban geometry, and city structure [11–13]. The rapid urban growth has entailed the absorption of urban heat, exerting a considerable impact on urban-scale climate variations [14]. Consequently, the continuous transformation of urban form and function has led to modifications in urban climate conditions. Due to the swift transformation of LULC and the elevated population density within urban areas of developing nations, these cities are becoming increasingly susceptible [15,16]. The ultimate consequence of this transition is closely linked to changes in climate at the city scale and an escalation in human health risks [17–19]. Despite these challenges, developing

countries lack standardized urban morphology data and LULC information at the city scale. In China, climate-related research data and information are not readily accessible to the public, and data collection for urban morphology lacks uniform standards.

Climate change is a global challenge, with urban areas playing a central role in addressing it. Specifically, in developing countries, China's urbanization rate had reached 60.6% by the end of 2019, and it is projected to reach 65.5% by 2025 [20]. However, over four decades of rapid urbanization because of China's reform and opening-up policies have placed immense pressure on the urban living environment. Natural ecosystems have been supplanted by buildings and hard surfaces, disrupting the dynamic equilibrium of urban ecosystems. This, combined with other human activities, has led to continuous alterations in local urban thermal environments, giving rise to the urban heat island effect. This effect has had a profound adverse impact on urban air quality, haze control, and plant health. The urban heat island effect has prompted elevated energy consumption and heat emissions, contributing to the exacerbation of greenhouse gas emissions, thereby intensifying global climate change and ecological degradation. This, in turn, affects urban economic development and public health. Therefore, taking actions to enhance urban thermal environments, representing urban climate governance, is of utmost significance for mitigating global climate change and aligning with the national "urban climate adaptation" action strategy.

1.2. Role of LCZ in Urban Climate Research

In this context, Stewart and Oke's (2012) concept of the LCZ and the associated climate-related classification based on homogeneous urban structures and land cover have become widely discussed and more reliable schemes for categorizing urban underlying surfaces. The LCZ is comprised of 17 distinct and mutually exclusive urban landscape categories that provide more detailed urban and suburban environmental information, particularly within the city core. These urban landscape categories are based on the nature, structure, material, and human activities on the land surface. The definition of LCZ types is closely related to physical surface features such as roughness, albedo, and anthropogenic heat outputs. This physical information serves climate researchers more effectively. LCZs essentially represent an improved Land Use/Land Cover (LULC) classification system, where each LCZ category aggregates information about the physical properties and the geometry, thermal, radiative, and land surface cover characteristics of built-up areas or natural land cover types. The LCZ offers a non-overlapping and complementary landscape zoning, encompassing the major urban morphological and land cover types.

Recent research related to the LCZ has been widely applied in three major areas [10,14]: (i) the development of cross-city LCZ maps, (ii) the application of the LCZ classification schemes in urban planning and urban climate management, and (iii) the assessment of the LCZ classifications through field observations. Presently, the LCZ schemes have been used to scrutinize the temperature and built environment patterns of different cities in various climatic regions worldwide [21,22]. Furthermore, the LCZ schemes have proven highly beneficial in comprehending the spatial distribution of thermal environments related to LULC changes and urban climate conditions [23,24]. At present, the LCZ is being extensively used in meso- and micro-scale research. For example, LCZs have been employed in predictive studies and in conjunction with other methods to investigate urban thermal environments and outdoor temperatures in urban areas [25,26]. The LCZ schemes are also given priority in climate modeling simulations for urban heat islands (UHI) research. In many previous studies, it was widely acknowledged that land cover is a crucial determinant of UHI distribution and land surface temperature (LST) in any area is largely influenced by the density and land cover area [27–30]. Thus, investigating the cross-city temperature and built environment patterns on different LCZs is crucial for improved urban climate management. Additionally, Ayman Aslam and Irfan Ahmad Rana's research has contributed significantly to our understanding of LCZ and its applications in urban climate research [31]. Their systematic review provides valuable insights into data

sources, methods, and themes related to the LCZ, which have further enriched the body of knowledge in this field.

1.3. LCZ Classification Methods and Statistical Units

LCZs have been introduced as a refined urban surface classification system, as proposed by Stewart and Oke in 2012. The LCZ categorizes urban areas into 17 distinct climate zones based on parameters influencing the urban heat island effect, such as building density, surface reflectance, sky view factor, and surface roughness length [2]. The primary purpose of the LCZ is to standardize climate observations and facilitate global climate research exchange. The LCZ has various applications, including guiding the placement of urban meteorological stations and human comfort monitoring points, assisting in the standard reporting and comparison of urban heat island effects between different cities, establishing objective criteria for measuring the intensity of urban heat islands, and guiding exploratory investigations into the causes and control factors of heat islands.

There are three main methods for the LCZ classification, namely supervised manual classification, remote sensing image recognition, and GIS-based urban spatial databases [32]. The GIS-based method is a commonly employed technique for mapping LCZs. Since the initial descriptions by Lelovics et al. [4] and Unger et al. [33] regarding GIS-based approaches for deriving LCZ maps, several representative GIS-based studies have been published [34]. Based on seven spatial features, Estacio et al. [35] classified the LCZ of Quezon City, Philippines, using a fuzzy logic algorithm and cellular automaton. Hidalgo et al. [36] applied the k-means clustering method to determine the boundaries of compact and open LCZ categories. Additionally, there are studies that utilize k-means clustering to identify LCZ types [37,38]. Since metadata in GIS methods is derived from actual urban morphology, these methods often achieve high precision and accuracy. However, not every city's spatial data and information are complete or accessible to the public, especially in developing countries and regions [39]. This pixel-based remote sensing (RF) supervised method has been integrated into the World Urban Database and Access Portal Tools (WUDAPT) for some European countries. Currently, many researchers worldwide are applying the WUDAPT method in their studies [40,41]. The LCZ maps generated through the RF and GIS-based methods have been subject to comparative studies in several cities [39,42,43]. Apart from differences in the classification process, these two types of LCZ mapping methods also exhibit variations in accuracy and types of classification [44]. Generally, the accuracy of RS-based methods depends on the selection of LCZ training samples, chosen based on the standards defined by Stewart and Oke (2012) [2]. In contrast, GIS-based methods often introduce or define new LCZ categories or subclasses [45].

The GIS-based urban spatial database method, on the other hand, requires more urban spatial and planning data support, involves greater computational effort, and is time-consuming. However, this method enhances data accuracy by quantifying urban spatial information and allows for the precise identification of different land surface types within cities. It can be adjusted and optimized according to the specific characteristics of urban underlying surfaces, making it particularly suitable for urban climate planning and decision making, facilitating alignment with a city's development control system.

In terms of statistical units for the LCZ classification, two methods are commonly employed: vector units and raster units. In this study, we use blocks as the smallest statistical unit for LCZ classification, based on urban spatial indicators and supervised classification methods. Although this approach may lack uniform geographical precision, blocks bound by urban road networks have a significant advantage in capturing the shape of objects. They can adhere to the precise boundaries of land cover elements, aligning with the customary practice of Chinese urban planning, which uses street boundaries as management units. Moreover, this approach facilitates subsequent supervision and management by urban planning scholars.

1.4. Research Objectives

This study has the following clear and straightforward research objectives:

1. To enhance local climate zoning in Xi'an by utilizing land parcels as the foundational statistical units. This will involve revising existing criteria to better align with the unique urban spatial planning features of Xi'an. We employ two distinct classification methodologies: one based on urban spatial indicators and supervised classification, and another reliant on urban morphology indicators, employing spatial clustering techniques to categorize surface attributes within the Xi'an region.
2. To evaluate these two classification methods and determine the most suitable approach for urban local climate zoning in Xi'an. This evaluation not only assesses the compatibility of the local climate zoning hierarchical system but also explores the spatial distribution characteristics of local climate zoning within the Xi'an urban area.

In this introduction, we emphasize the paramount importance of comprehending urban climates for the effective undertaking of urban planning and climate studies. We introduce the concept of Local Climate Zones (LCZs), a systematic classification framework that demarcates urban areas into 17 specific zones based on factors influencing the urban heat island effect. The LCZ offers a multitude of pragmatic applications in urban planning, facilitating the strategic placement of weather stations, and standardizing the reporting of climate data.

The concluding portion of this introduction delves into the profound implications of urbanization on the urban climate and underscores the pivotal role that LCZ plays in the realm of urban climate research. The process of urbanization has precipitated substantial modifications in land use and land cover, exerting a significant impact on local climate conditions. Within the Chinese context, the rapid pace of urbanization presents multifaceted challenges, encompassing issues related to urban climate governance and environmental quality. As a classification system, LCZ furnishes a robust framework that underpins our understanding of urban climates. Recent research attests to the versatility of LCZ, as it finds application in diverse domains, encompassing urban planning, climate management, and the nuanced analysis of thermal environments. Subsequently, our attention shifts to the methods employed in the LCZ classification and the selection of statistical units. Here, we accentuate the pragmatic merits of the GIS-based approach, with a particular emphasis on the utilization of "blocks" as the smallest statistical unit. This method excels in ensuring the meticulous identification of various land surface types within urban areas. It aligns harmoniously with the conventions of Chinese urban planning practices, notably the utilization of street boundaries as management units.

In the pursuit of our research endeavors, we aspire to scrutinize the applicability of the LCZ classification within the urban landscape of Chinese cities, with a specific focus on those characterized by high population density. This undertaking is poised to contribute significantly to the enhancement of our comprehension concerning the potential of the LCZ in the realm of urban climate studies and urban planning. Such contributions are especially pertinent in the context of regions undergoing rapid urbanization, typified by the scenario prevalent in China.

2. Materials and Methods

2.1. Research Area

Xi'an city, located in the central–northwestern region of China (Figure 1), emerges as a formidable historical and cultural entity, in addition to its substantial economic significance. It is noteworthy not only for being one of the most ancient continuously inhabited cities globally but also for its historical role as the capital of various Chinese dynasties, such as the Western Zhou, Qin, Han, and Tang. These legacies have indelibly imprinted themselves upon its urban and architectural landscape, enriching its historical tapestry.

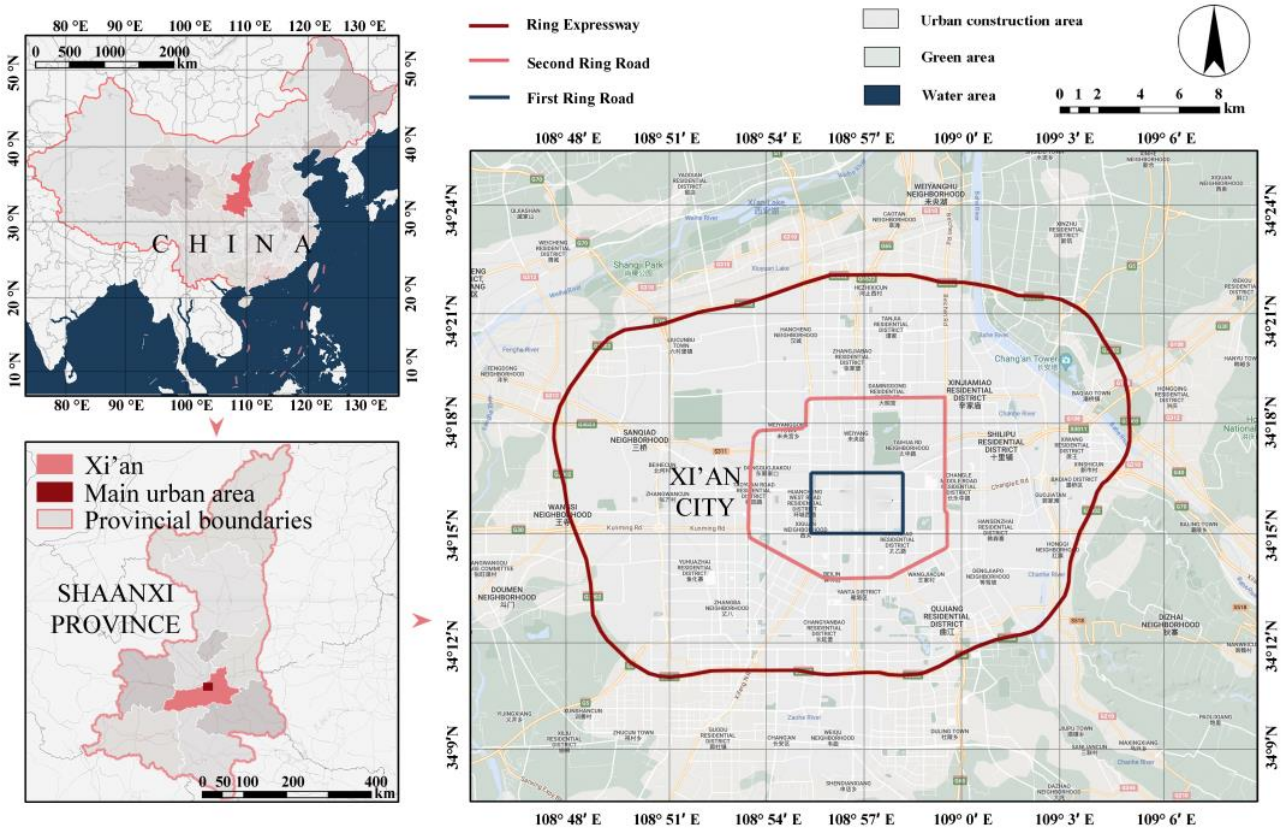


Figure 1. Geographical Location Map of Xi'an.

Geographically, Xi'an is situated in Guanzhong Plain, enveloped by the Qinling Mountains to the south and the Wei River to the north. This geographical positioning results in a distinctive combination of natural attributes, ranging from fertile plains to picturesque mountain ranges. This diversity in topography significantly shapes the local climate zones in Xi'an, subjecting them to an array of microclimatic influences.

Recent years have witnessed a swift process of urbanization in Xi'an, leading to notable transformations in land use, urban morphology, and the thermal environment. It has now become imperative to comprehend the intricate fabric of local climate zones within the city, with implications for sustainable urban planning, climate mitigation strategies, and the amelioration of the quality of life for urban residents.

This research introduces a pioneering methodology for categorizing Xi'an city's local climate zones. This method leverages spatial indicators and supervised classification techniques to create a nuanced understanding of these zones. By scrutinizing the intricate interplay of geographical and meteorological factors, this research aims to provide invaluable insights into the microclimates of the city. Ultimately, it seeks to assist in the formulation of climate-responsive urban policies, fostering the creation of more sustainable and habitable urban environments within Xi'an.

2.2. Data Sources and Indicator Calculation Methods

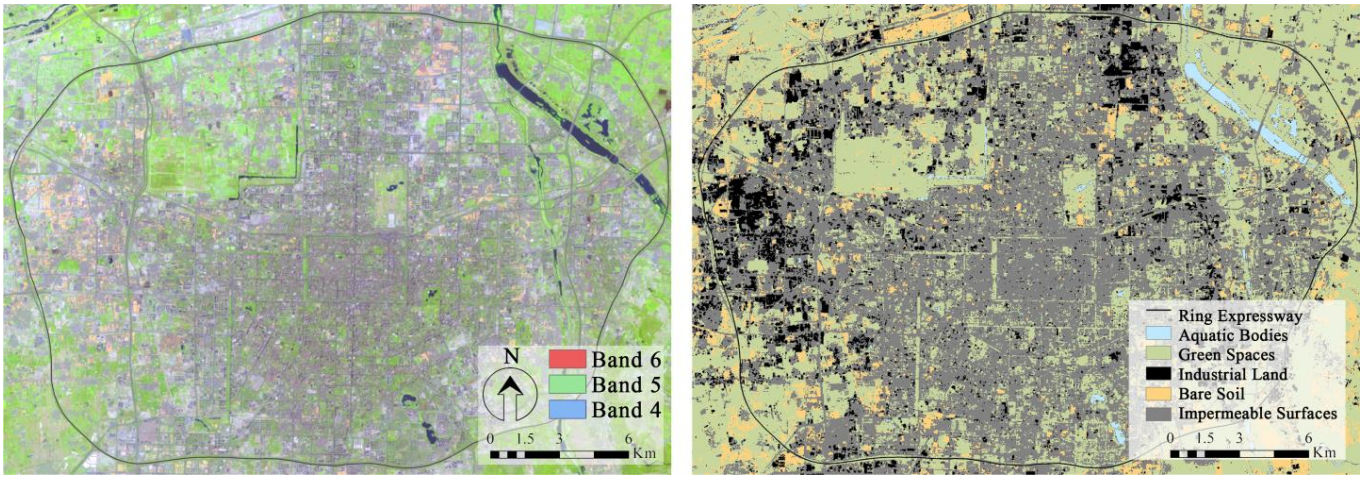
2.2.1. Underlying Surface Indicators

The underlying surface structure category indicators pertain to urban land surface cover conditions. In the present investigation, the land surface cover within the research area underwent classification into five distinct categories through the utilization of a supervised classification method reliant on remote sensing image attributes, as exhaustively delineated in Table 1. This categorization, as illustrated in Figure 2, encompasses the following classes: impervious surfaces (comprising areas dominated by rigid surfaces such as conventional buildings, paved pathways, road networks, and the like), soil and bare

land (encompassing undeveloped and open land parcels), water bodies (comprising all aqueous surfaces, including rivers, lakes, canals, and fountains), green spaces (inclusive of vegetated zones, encompassing trees, and regions marked by substantial vegetal shading), and light industrial land (embodying areas featuring lightweight roofing materials within structures designed in an industrial shed-style architecture).

Table 1. Classification Method and Procedure for Land Cover.

Primary Steps	Description	Tools Used
Band Synthesis	Synthesize Landsat 8 remote sensing image data's bands 7, 5, and 3 into a single raster image.	Band synthesis
Training Sample Creation	Create training sample areas for impermeable surfaces, bare soil, water bodies, green spaces, and industrial land. Ensure even distribution within the study area.	Image classification
Supervised Classification	Employ an algorithm based on spectral information to cluster the pixels in the raster image according to the classification rules defined by the training sample areas.	Maximum Likelihood method
Post-Classification Processing	Utilize boundary cleaning and mode filtering to smooth small patches or region edges in the image.	Mode filtering
Classification Accuracy Assessment	Evaluate the accuracy of the classified raster image, resulting in a classification accuracy of 88% and a Kappa index of 0.85, demonstrating a reasonable classification.	Accuracy, Kappa coefficient



(**a**) (**b**)

Figure 2. Land Cover Image Maps: (**a**) Original Downloaded Raster Image; (**b**) Supervised Classification Resulting in Spatially Classified Raster Image of Xi'an City Land Cover.

2.2.2. Street Block Three-Dimensional Morphology Indicators

This study primarily focuses on assessing urban block morphology through spatial indices, with particular emphasis on building density and building height. Building density, a fundamental indicator of urban block morphology, is determined by the ratio of total built-up area to the total land area within a given block. Building height, another vital aspect of urban block morphology, is assessed by measuring the average height of structures within the block. The computation methods and corresponding formulas for these indices are comprehensively detailed in Tables 2 and 3.

Table 2. Calculation Methods for General Morphological Indicators.

Indicators	Indicator Description and Calculation Method	Data Source
Building Density (%)	Sum of the footprint areas of all buildings/Total area of the parcel	Urban Spatial Model
Building Height (m)	Average height of all buildings within the parcel, total volume of all buildings/Sum of footprint areas of all buildings	Urban Spatial Model

Table 3. Formulas for General Morphological Indicators.

Indicators	Formula	Coefficient Description
Building Density	$BD = \frac{\sum_{i=1}^{n} BS_i}{S_{block}}$	BD refers to building density. BS_i represents the footprint area of building *i*. S_{block} denotes the parcel area. *n* signifies the total number of buildings within the parcel.
Building Height	$BH = \frac{\sum_{i=1}^{n} V_i}{\sum_{i=1}^{n} BS_i}$	BH signifies building height. V_i indicates the volume of building *i*. $\sum_{i=1}^{n} BS_i$ represents the total footprint area of all *n* buildings within the parcel.

2.3. Classification of Local Climate Zones in Xi'an Based on Urban Spatial Indicators and Supervised Classification

LCZs are categorized into two primary classes: built-up coverage and natural land cover. Under this framework, built-up areas are further subcategorized into 10 distinct types, while natural land covers are delineated into 7 types, resulting in a total of 17 LCZs, as exemplified in Figure 3 [2].

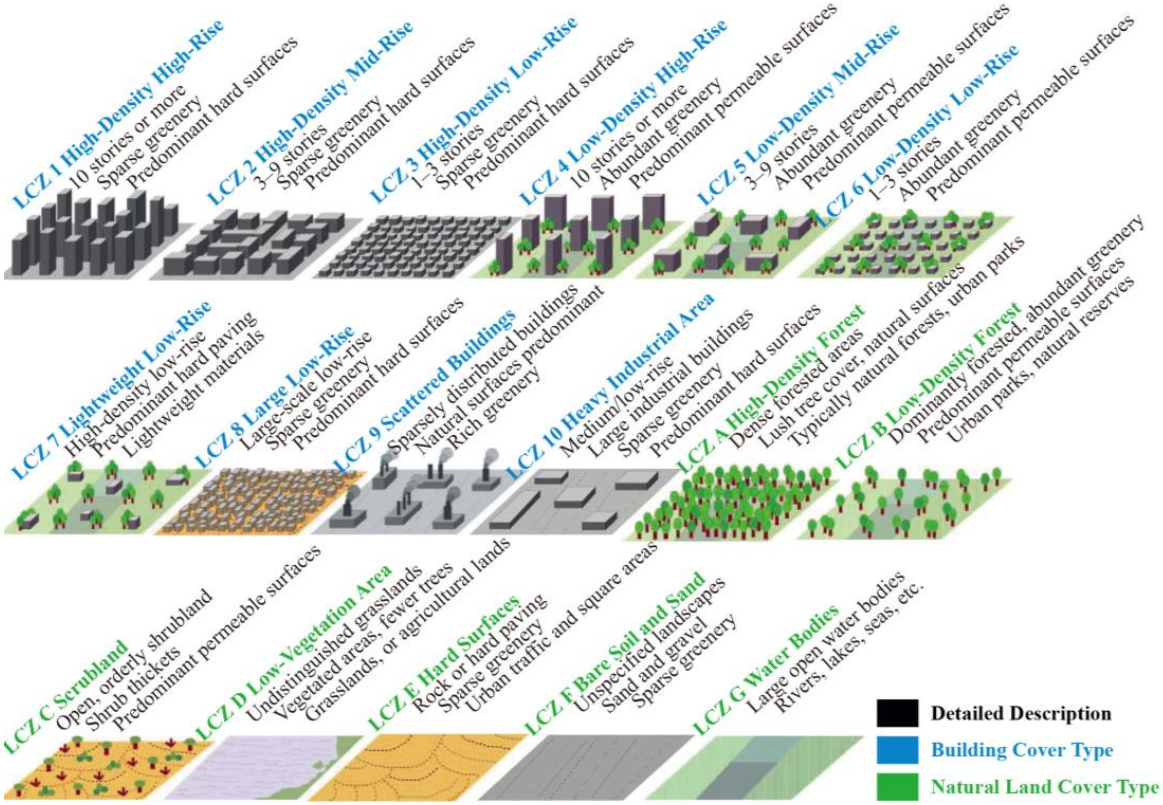


Figure 3. Local Climate Zone Classification and Definitions Proposed by Stewart and Oke.

Initiating the classification procedure, land parcels characterized by natural land cover (LCZ A, B, C, D, E, F, G) within the urban setting are delineated. Leveraging spatial data on green spaces, bodies of water, soil composition, pavement ratios in Xi'an, in conjunction with land use characteristics, Google Maps, and street view data, a decision tree is formulated for the classification of natural land cover into LCZs, as depicted in Table 4. It is pertinent to note that within the primary urban area of Xi'an, there are no densely forested regions or clearly defined low shrub areas, rendering LCZ A and LCZ C absent from the study area. As for the LCZ D category, which characterizes areas with low vegetation, it is further subdivided into LCZ D and LCZ D-II based on the health of plant growth and the level of greening within land parcels.

Table 4. Decision Tree for Local Climate Zone Classification of Natural Features.

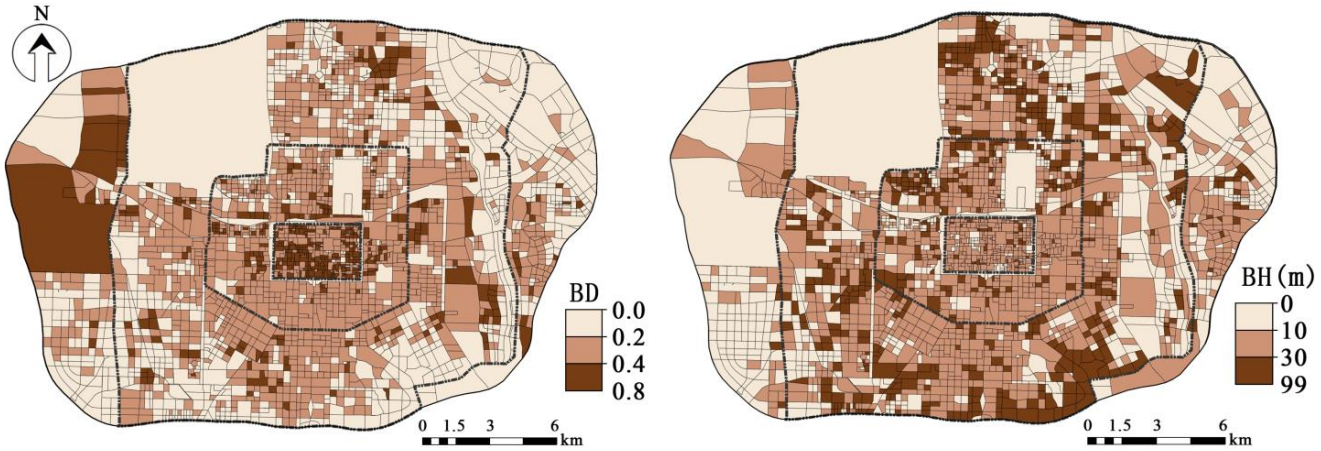
LCZ Category	Classification Criteria	Land Use
LCZ B	Greenery Ratio > 0.7 with Predominance of Tall Vegetation in Urban Parks	Green Spaces
LCZ D	Building Density = 0; Greenery Ratio > 0.5, Predominantly Lawns and Farmland	Green Spaces
LCZ D-II	Building Density = 0; Greenery Ratio < 0.5	Green Spaces
LCZ E	Paved Surface Ratio > 0.7, Mainly Utilized for Transportation or Plazas	Other
LCZ F	Bare Soil Ratio > 0.7, Predominantly in Urban Open Areas	Other
LCZ G	Water Body Ratio > 0.7, Primarily Comprising Rivers and Water Bodies	Water Bodies
LCZ D	Building Density = 0; Greenery Ratio > 0.5, Predominantly Lawns and Farmland	Green Spaces

Moving forward, land parcels exhibiting distinct built-up coverage (LCZ 7, 8, 9, 10) within the urban context are classified. Utilizing data from the preceding section, encompassing Xi'an's industrial proportions and 3D urban models, alongside land use characteristics, Google Maps, and street view data, a decision tree is established to classify specialized built-up coverage into LCZs, as delineated in Table 5. Notably, there are no areas designated for heavy industrial use within the primary urban area, rendering LCZ 10 inapplicable. Moreover, isolated built-up areas under a natural vegetation canopy (LCZ 9) are non-existent within the study area, leading to the exclusion of LCZ 9 during the classification process.

Table 5. Decision Tree for Local Climate Zone Classification of Special Building Cover Types.

LCZ Category	Classification Criteria	Land Use
LCZ 7	Industrial Ratio > 0.7; Building Height < 10 m, Predominantly Lightweight Materials such as Prefabricated Structures	Industrial
LCZ 8	Large-Scale Buildings with Area > 7000 m^2 and Height < 10 m	Industrial/Commercial

Subsequently, land parcels characterized by built-up coverage (LCZ 1, 2, 3, 4, 5, 6) are subjected to classification. Following the LCZ classification standard [2], built-up areas are categorized into six classes based on three building height levels (high, medium, and low) and two building density conditions (compact and spacious). However, this classification system, originally developed for European cities, does not seamlessly align with the unique characteristics of Chinese cities, particularly in light of China's rapid urbanization and the intricate urban land patterns found in Xi'an. The prevailing LCZ classification only distinguishes between compact and spacious building densities, which fails to correspond with the more granular density categories present in China's urban planning system. In response, the initial step involves categorizing building density and height into high, medium, and low levels, in accordance with established Chinese conventions, as outlined in Figure 4.



(**a**) (**b**)

Figure 4. Spatial Grading Map of Building Density and Building Height (General Building Cover Types) (**a**) Local Climate Zone (Building Density) Spatial Grading Map; (**b**) Local Climate Zone (Building Height) Spatial Grading Map.

Building upon the Stewart and Oke's LCZ classification standards, further sub-classification is applied to LCZ 4, LCZ 5, and LCZ 6, which are classified as spacious building density types. These are subdivided into LCZ 4 and LCZ 4-II (low-density high-rise and medium-density high-rise), LCZ 5 and LCZ 5-II (low-density mid-rise and medium-density mid-rise), and LCZ 6 and LCZ 6-II (low-density low-rise and medium-density low-rise), thereby introducing three subtypes to accommodate the substantial variations in building density found within the study area. The revised classification standards for LCZs within built-up areas (LCZ 1–6) are presented in Table 6.

Table 6. Decision Tree for Local Climate Zone Classification of Natural Features.

Category	Classification Criteria	Building Density	Building Height
LCZ 1	High-Density High-Rise	Building density $\geq$ 0.4	Average height $\geq$ 30 m (10 stories or more)
LCZ 2	High-Density Mid-Rise	Building density $\geq$ 0.4	10 $\leq$ Average height < 30 m (3–9 stories)
LCZ 3	High-Density Low-Rise	Building density $\geq$ 0.4	Average height < 10 m (1–3 stories)
LCZ 4	Low-Density High-Rise	Building density < 0.4	Average height $\geq$ 30 m (10 stories or more)
LCZ 4-II	Medium-Density High-Rise	0.2 $\leq$ Building density < 0.4	Average height $\geq$ 30 m (10 stories or more)
LCZ 5	Low-Density Mid-Rise	Building density < 0.4	10 $\leq$ Average height < 30 m (3–9 stories)
LCZ 5-II	Medium-Density Mid-Rise	0.2 $\leq$ Building density < 0.4	10 $\leq$ Average height < 30 m (3–9 stories)
LCZ 6	Low-Density Low-Rise	Building density < 0.4	Average height < 10 m (1–3 stories)
LCZ 6-II	Medium-Density Low-Rise	0.2 $\leq$ Building density < 0.4	Average height < 10 m (1–3 stories)

2.4. Classification of Local Climate Zones in Xi'an Based on Spatial Clustering Analysis Methods

This study applied spatial clustering analysis methods to classify individual building characteristics, namely building density and building height, into seven distinct groups with the objective of optimizing intra-group feature uniformity while maximizing inter-group feature diversity. The research employed the widely accepted k-means clustering method in cluster analysis and subsequently evaluated the validity of building classification through ANOVA testing, as presented in Table 7. The findings reveal that the land parcels containing various building types within Xi'an city have been effectively segmented into seven distinct categories, as illustrated in Table 8.

Table 7. Analysis of Variance (ANOVA) Results Table.

ANOVA							
	Clustering		Error		F	Significance	*p*-Value
	Mean Square	Freedom Degrees	Mean Square	Freedom Degrees			
Building Height	120,413.137	6	10.405	2311	11,572.515	0.000	<0.001
Building Density	0.550	6	0.016	2311	34.517	0.000	<0.001

Table 8. Spatial Clustering Results Table.

Final Clustering Center							
	Clustering						
	1	2	3	4	5	6	7
Building Height	91.56	8.69	58.85	28.81	73.20	41.66	18.29
Building Density	0.17	0.30	0.20	0.27	0.19	0.22	0.33
Classification Criteria	L-D H-R	H-D L-R	M-D SH-R	SH-D M-R	L-D SH-R	M-D M-R	H-D M-R
Local Climate Zone	LCZ 4	LCZ 3	LCZ 5-III	LCZ 2-II	LCZ 4-II	LCZ 5-II	LCZ 2

Abbreviations: L-D: Low-Density, M-D: Medium-Density, SH-D: Sub High-Density, H-D: High-Density. L-R: Low-Rise, M-R: Low-Rise, SH-R: Sub High-Rise, H-R: High-Rise.

3. Results and Discussion

3.1. Spatial Distribution Characteristics of Local Climate Zones in Xi'an City

3.1.1. Local Climate Zone Based on the Supervised Classification Method

Utilizing a decision tree rooted in the proposed LCZ classification standards, we executed a spatial classification of building coverage and land cover types within Xi'an. Subsequently, these classifications underwent spatial integration, bolstered by meticulous manual supervision, culminating in the creation of a bespoke LCZ map that accurately reflects the urban development and spatial intricacies of Xi'an's primary urban region, as visually represented in Figure 5.

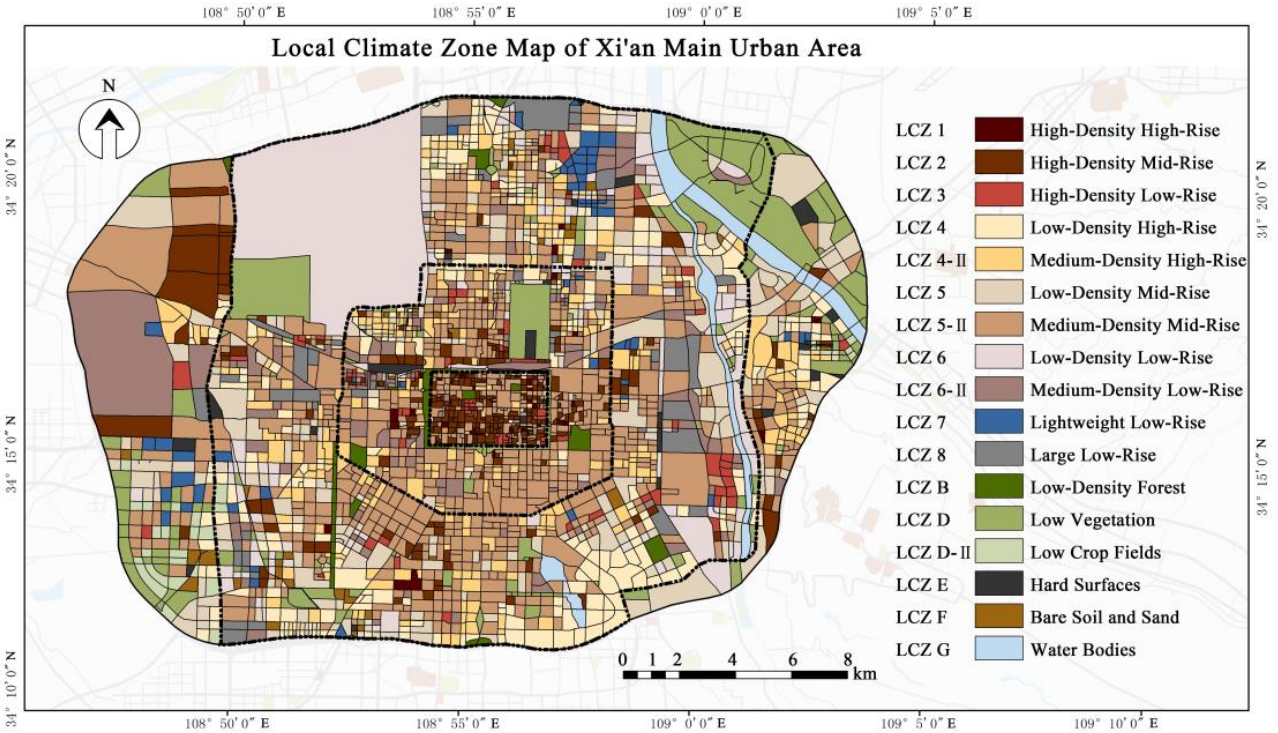


Figure 5. Local Climate Zone Map of Xi'an Main Urban Area by Supervised Classification Method.

Xi'an exhibits notable spatial variations in its LCZs. Generally, the central city area is characterized by a preponderance of built-up coverage, while the peripheral zones predominantly feature natural land covers. The LCZ 5-II (medium-density mid-rise) category emerges as the most pervasive spatial typology within Xi'an's main urban area, encompassing approximately 30% of the total land parcels (Figure 6). It is primarily situated between the first and second ring roads, extending beyond the second ring road, and is notably concentrated in older residential neighborhoods and substantial educational institutions. Following closely, the LCZ 4-II (medium-density high-rise) classification constitutes the second most prevalent type, accounting for 11% of the total land parcels. These areas are primarily located between the second and third ring roads and are frequently observed in high-rise residential sectors and high-rise office districts, mirroring a prominent urban development trend within Xi'an in recent years.

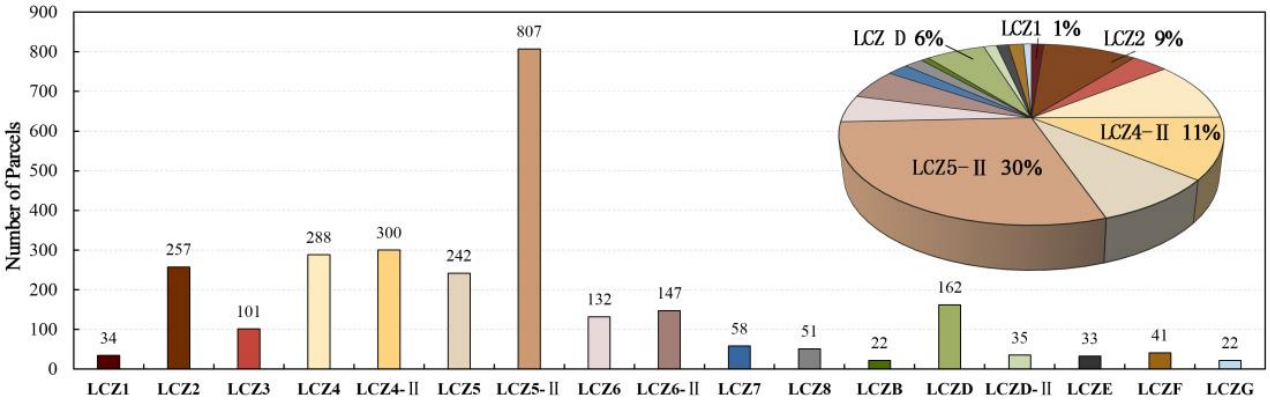


Figure 6. Statistics of the Number and Proportions of Different Local Climate Zone Categories.

In general, high-rise residential buildings in Xi'an adhere to daylight design standards, advocating for ample spacing between structures to accommodate an abundance of green vegetation coverage and enhance outdoor thermal comfort for residents. However, to address the demands of urbanization and population density, plot ratios have escalated, resulting in heightened building densities within high-rise residential areas in Xi'an. Consequently, medium-density types predominate within these areas, with only a limited number of low-density high-rise buildings (LCZ 4) situated in the city's peripheries, such as around Qujiang Pool Ruins Park in the southeast and the Baqiao Wetland in the northeast, signifying upscale residential enclaves.

High-density areas (LCZ 1, LCZ 2, LCZ 3) are chiefly clustered within the ancient city enclosed by the first ring road and in the northwestern industrial zones. Predominantly, LCZ 2 (high-density mid-rise) accounts for 9% of the total land parcels. This concentration arises from the constraints on building height within the first ring road, leading to primarily mid to low-rise structures with extensive building footprints and compact layouts. Consequently, the region enclosed by the first ring road emerges as the highest-density sector in Xi'an. High-density high-rise areas (LCZ 1) represent a mere 1% of the total, distinguishing Xi'an's main urban area from high-density high-rise metropolises like Hong Kong and Tokyo and accurately positioning Xi'an's central urban region as predominantly characterized by high-density mid-rise structures.

Furthermore, specialized building coverage types, such as lightweight construction (LCZ 7), are relatively scarce, primarily concentrated in industrial areas on the city's periphery or construction sites. Areas with substantial vegetation (LCZ B) are sporadically dispersed throughout various city zones, albeit in limited numbers. Low-lying vegetation areas (LCZ D) account for a slightly larger proportion, amounting to 6%, and are predominantly clustered in the city's northeast and southwest corners. Xi'an, being an inland city with few natural water bodies, boasts only a handful of water bodies, notably the Wei River, Ba River, and artificial water bodies like the Qujiang Pool and Xingqing Palace.

Impervious surfaces (LCZ E) are commonplace at transportation hubs, train stations, and paved squares within the city. Bare soil and sand (LCZ F) areas are primarily found in undeveloped regions and exposed agricultural fields.

In summary, Xi'an's urban development has steadily extended from the inner city to its peripheries, continuously progressing along the central axis from south to north. The defining feature of Xi'an's urban landscape within the primary urban area is the prevalence of medium-density mid-rise and medium-density high-rise building types. This study has meticulously refined the existing LCZ classification standards, considering the unique attributes of Xi'an's urban development, and meticulously delineated building coverage types in alignment with common Chinese urban planning practices. This adaptation aims to provide a rigorous foundation for classifying the urban morphology of Xi'an's primary urban area from the perspective of thermal environmental considerations.

3.1.2. Local Climate Zone According to the Clustering Classification Method

The results obtained through clustering classification differ from those obtained via supervised classification. High-density mid-rise (LCZ 2) and high-density low-rise (LCZ 3) emerge as the most predominant spatial categories within the central urban area, collectively constituting approximately 53% of the total land parcels. They encompass virtually all of the older urban zones and extend beyond the second ring road. Subsequently, sub-high-density mid-rise (LCZ 2-II), which primarily intermingle between LCZ 2 and LCZ 3, exhibit wide distribution within the areas situated between the first and second ring roads, as well as between the second and third ring roads, with extensions even beyond the third ring road.

These three primary spatial categories collectively account for roughly 68% of the total land parcels. In stark contrast to the results of supervised classification, the medium-density mid-rise (LCZ 5-II) category comprises a relatively minor proportion, approximately 7%. A novel category, LCZ 5-III, has been introduced to denote medium-density sub-high-rise, with a proportion of 5%. These are predominantly situated between the second and third ring roads and are commonly found in older residential neighborhoods within the urban area and at institutional locations, such as colleges and university faculty housing complexes.

From Figure 7, it is discernible that the utilization of a spatial clustering methodology for the demarcation of Local Climate Zones (LCZs) in Xi'an yields a predominant classification of land parcels as possessing medium to high density and medium to low height characteristics. This approach proves inadequate in capturing the diverse spectrum of land parcel types that exist throughout the entire study area. Moreover, the centroids and threshold ranges associated with the seven LCZs, as determined through the k-means clustering method, exhibit a significant departure from the established classification norms within the realm of Chinese urban planning. Some threshold ranges for spatial morphology classification are challenging to correspond to appropriate urban block types. As shown in Table 8, according to urban planning conventions, when the center point of Building Height is 41.66 m and Building Density is 0.22, it is considered as Medium-Density Mid-Rise. When Building Height is 28.81 m and Building Density is 0.27, it can still be classified into the broader category of Medium-Density Mid-Rise. Theoretically, the Building Density exceeding 0.4 belongs to the High-Density category. While in the clustering process, it is difficult to precisely align the classification results with planning conventions. Building Density of 0.33 and 0.3, can be classified as High Density. According to statistics, there are 781 blocks in Xi'an with an average building density between 0.2 and 0.3, accounting for 28% of the total, which is a substantial proportion. Therefore, we classified blocks with BD = 0.27 and BH = 28.81 as Sub High-Density Medium-Rise (LCZ 2-II) to avoid grouping too many blocks into the same category, making it challenging to capture spatial morphological differences. Nevertheless, even with this adjustment, the LCZ classification obtained through clustering still differs significantly from urban planning conventions. Consequently, the practical application of this LCZ classification framework in the context of urban planning and urban

climate management in Xi'an becomes exceedingly challenging. Hence, it is imperative to consider an alternative approach, one rooted in spatial index-based and supervised classification methods, as being better suited for the delineation of Local Climate Zones in Xi'an.

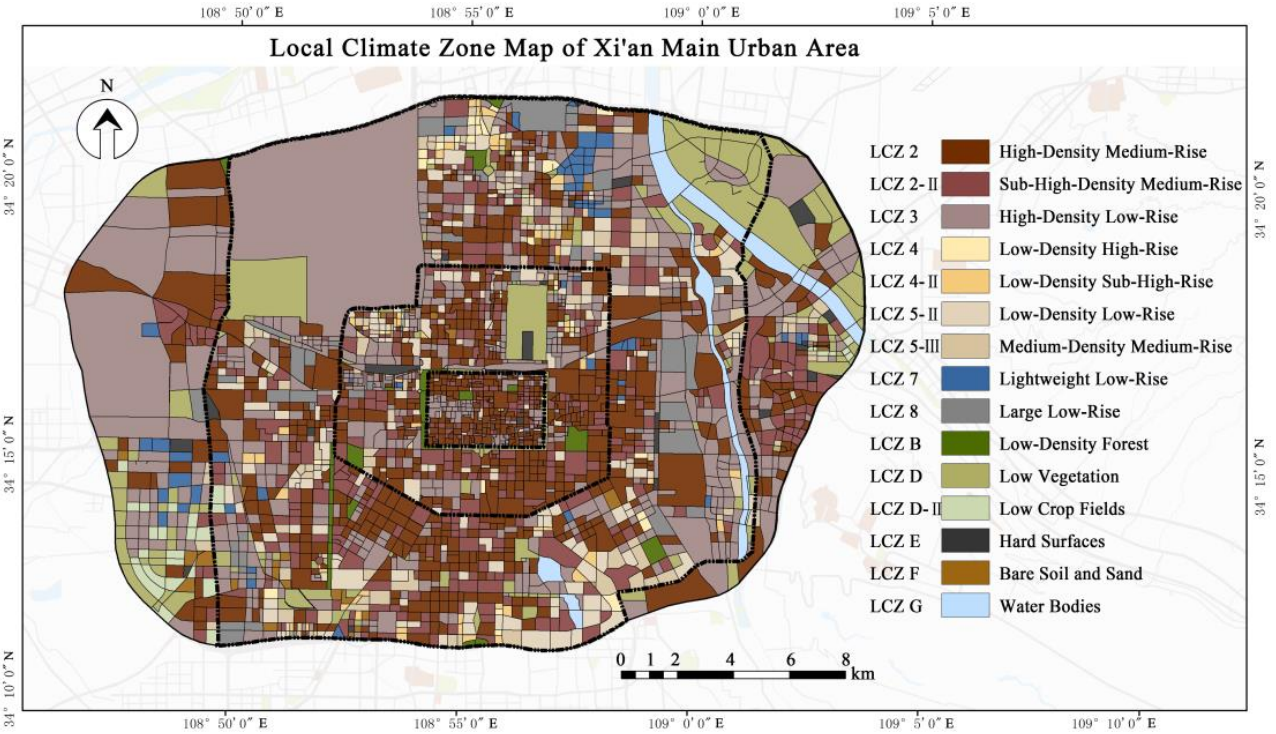


Figure 7. Local Climate Zone Map of Xi'an Main Urban Area by Clustering Classification Method.

3.2. Performance Evaluation of the Improved Local Climate Zone System in Xi'an

In accordance with Stewart and Oke's LCZ classification standards and guidelines [2], each LCZ category is associated with four distinct aspects encompassing a total of ten thermal environment-related indicators. These aspects include surface structure, involving the parameters sky view factor (SVF), height-to-width ratio (H/W), mean height (BH), and roughness (ROU); land cover, comprising building density (BD), impervious surface fraction (PSF), and permeable surface fraction (TSF); surface materials, characterized by reflectance (P_R) and surface albedo (SA); and human activities, encapsulating anthropogenic heat flux (BAH). The range of values assigned to these indicators is primarily derived from a comprehensive synthesis of existing research, empirical data, and measurements [5].

In this research, the local climate zones (LCZs) in Xi'an were categorized into either 9 or 7 building types, with land parcels as the statistical unit. Employing the spatial indicators calculated in Section 2.2 and certain urban spatial morphology data [46], 10 spatial indicators with verification attributes were extracted. Subsequently, for each category, calculations were executed for the ten urban spatial indicators, yielding quartiles (first, second, and third quartiles) for these parameters, as detailed in Tables 9 and 10. This analytical approach enabled the quantification of surface structure, land cover, surface materials, and human activities within the 9 or 7 LCZ categories, thereby validating the suitability of the enhanced urban LCZ system in Xi'an.

As shown in Table 9, the statistical outcomes closely conform to the LCZ attributes proposed by Stewart and Oke [2]. In essence, substantial differences in urban attributes are discernible among diverse LCZ categories, while disparities within the same category are relatively minor. This achievement holds paramount significance in achieving a judicious classification of urban spaces from a climatic perspective.

Table 9. Range of Values for Different Local Climate Zones (LCZ1-LCZ6) in Urban Attributes.

Indicators	LCZ1	LCZ2	LCZ3	LZC4	LCZ4-II	LCZ5	LCZ5-II	LCZ6	LCZ6-II
SVF	0.4–0.7 0.55	0.4–0.8 0.54	0.4–0.8 0.64	0.6–0.9 0.81	0.5–0.86 0.67	0.7–0.9 0.88	0.5–0.86 0.69	0.8–0.9 0.89	0.7–0.9 0.82
H/W	1.1–3.3 1.6	0.5–1.3 0.8	0.2–0.5 0.36	1.2–3.5 2.0	1.2–3.2 1.7	0.1–1.1 0.71	0.5–1.2 0.79	0.1–0.4 0.24	0.16–0.50 0.33
BH (m)	30–63 34	11–24 16	5–9 8	31–78 48	30–68 40	10–26 17	11–26 18	3–9 6	4–10 7
ROU	1–2 1	1–1 1	1–1 1	0.5–2 1	0.5–2 1	0.5–2 0.5	0.5–2 1	0.5–0.5 0.5	0.5–1 0.5
BD	0.4–0.5 0.45	0.4–0.6 0.45	0.4–0.7 0.50	0.1–0.2 0.15	0.2–0.3 0.26	0.1–0.2 0.15	0.2–0.4 0.29	0–0.18 0.10	0.22–0.37 0.29
PSF	0.1–0.4 0.29	0.1–0.4 0.32	0–0.41 0.25	0.2–0.7 0.5	0.3–0.6 0.5	0.1–0.6 0.40	0.2–0.6 0.42	0–0.56 0.28	0.05–0.56 0.39
TSF	0–0.12 0	0–0.1 0	0–0.12 0	0–0.6 0.24	0–0.32 0.06	0–0.66 0.35	0–0.42 0.13	0.1–0.9 0.47	0–0.51 0.15
P_R	0.1–0.2 0.15	0.1–0.19 0.16	0.1–0.18 0.14	0.24–0.28 0.26	0.2–0.3 0.23	0.2–0.3 0.26	0.18–0.24 0.22	0.24–0.29 0.26	0.19–0.25 0.21
SA	0.12–0.15 0.13	0.12–0.15 0.13	0.13–0.15 0.13	0.12–0.15 0.14	0.12–0.15 0.13	0.13–0.15 0.14	0.12–0.15 0.13	0.12–0.15 0.14	0.12–0.15 0.13
BAH (W/m^2)	422–1136 817	164–610 255	79–233 122	121–382 215	229–707 360	30–183 84	107–340 181	2–51 21	37–137 71

Table 10. Range of Values for Different Local Climate Zones (LCZ2-LCZ5-III) in Urban Attributes.

Indicators	LCZ2	LCZ2-II	LCZ3	LZC4	LCZ4-II	LCZ5-II	LCZ5-III
SVF	0.7–0.9 0.86	0.5–0.9 0.70	0.6–1.0 0.83	0.5–0.9 0.73	0.6–0.9 0.75	0.5–0.9 0.71	0.6–0.9 0.72
H/W	0.2–0.4 0.28	0.9–1.7 1.18	0.2–0.56 0.40	2.9–4.9 3.34	2.3–4.1 2.78	1.3–2.3 1.67	1.9–3.5 2.46
BH (m)	4–10 7	25–33 29	4–12 9	86–99 90	67–80 73	36–48 41	52–65 60
ROU	0.5–1 1	0.5–2 1	0.5–1 0.5	0.5–2 1	0.5–2 1	0.5–2 1	0.5–2 1
BD	0.3–0.6 0.36	0.1–0.4 0.26	0.4–0.7 0.29	0.1–0.3 0.15	0.1–0.3 0.19	0.1–0.3 0.21	0.1–0.3 0.19
PSF	0.0–0.5 0.34	0.2–0.6 0.43	0–0.5 0.34	0.2–0.6 0.53	0.3–0.7 0.54	0.2–0.6 0.48	0.2–0.6 0.51
TSF	0–0.6 0.13	0–0.4 0.13	0–0.6 0.14	0–0.5 0.14	0–0.4 0.07	0–0.5 0.12	0–0.6 0.15
P_R	0.1–0.2 0.20	0.2–0.3 0.23	0.1–0.3 0.22	0.2–0.3 0.25	0.2–0.3 0.26	0.2–0.3 0.24	0.2–0.3 0.25
SA	0.12–0.15 0.14	0.12–0.15 0.13	0.13–0.15 0.14	0.12–0.15 0.14	0.13–0.15 0.14	0.12–0.15 0.13	0.13–0.16 0.14
BAH (W/m^2)	32–224 121	131–584 240	14–214 86	215–1113 423	237–940 412	162–520 270	186–549 340

To illustrate, let us consider the high-density high-rise building type (LCZ 1). Evidently, its sky view factor is generally lower compared to other LCZ types, implying that outdoor spaces in LCZ 1 receive diminished solar radiation and, consequently, reduced exposure to solar radiation. Additionally, LCZ 1 exhibits a higher street canyon aspect ratio in comparison to other LCZ types. This discrepancy arises from the typical narrow street canyons in high-density high-rise areas, attributable to the towering building structures, resulting in larger aspect ratios. Furthermore, owing to the characteristics of high-density high-rise developments, LCZ 1 exhibits the highest anthropogenic heat intensity among the 9 LCZ categories.

From the data presented in Table 9, it is evident that, with the exception of surface albedo, the attributes exhibit marked inter-group distinctions across all LCZ categories.

However, in the LCZ zones delineated using spatial clustering methods (refer to Table 10), there is not a significant inter-group difference in some indicators, such as SA, P_R, SVF, ROU, and PSF. This indirectly indicates that clustering methods may not be suitable for partitioning LCZs in Xi'an.

In conclusion, the LCZ zones obtained through spatial metrics and supervised classification methods are better suited for Xi'an city. Each LCZ delineates specific ranges of sky view factor, aspect ratio, reflectance, roughness, anthropogenic heat, and underlying surface attributes. This empirical evidence underscores the effectiveness of the LCZ classification in rapidly unveiling urban form and structural characteristics, thus providing a preliminary insight into the spatial distribution of urban heat islands. This, in turn, facilitates a better grasp of the distinctive attribute features within each category, effectively translating abstract spatial data into an easily interpretable lexicon of urban morphology.

3.3. Comparison with Other Studies

Compared with the WUDAPT method, the GIS and supervised classification-based method is more accurate for classifying LCZs [32]. However, there are few studies that reported using a GIS-based method by employing large numbers of spatial indicators and supervised classification in developing LCZ maps at block level. It requires a substantial amount of urban spatial information data, morphological indicators, and more accurate land use data, as well as increased manpower input. Generally, spatial morphological data for large Chinese cities is often more readily available compared to smaller cities, with a moderate cost of data acquisition, providing researchers with possibilities for study. Some studies have already reported on the LCZ zoning methods for Xi'an. For instance, He Shan et al. [43] proposed a coupled classification method using the WUDAPT method and RF data, with vector road networks as statistical units for zoning, dividing Xi'an into 13 LCZ zones. Han Bing et al. [47] used the RF data to study the changes in LCZ zones in different periods in Xi'an. Both methods rely on the RF image datasets and the world database provided by WUDAPT, but the former aggregates data within vector blocks, while the latter uses raster units. In comparison, this study, based on multi-source data, calculated numerous spatial indicators, incorporated supervised classification, and finally improved the zoning criteria according to Chinese urban planning practices. The resulting LCZ classification method demonstrated improvements in both classification accuracy and applicability to subsequent urban planning and control.

4. Conclusions

In this research endeavor, an array of indicators sourced from Xi'an's urban spatial planning database was meticulously scrutinized. Employing a supervised classification methodology, the existing LCZ standards were refined. The ArcGIS platform was harnessed to systematically reclassify Xi'an's urban space through a tailored LCZ classification method that aligns with the distinctive high-density urban spatial development characteristics of the city. By leveraging the urban road network planning, land parcels were demarcated, facilitating the generation of a vector map of LCZs. This enhanced map is designed for seamless integration with subsequent urban planning endeavors, thereby facilitating more effective urban planning and control. Simultaneously, we endeavored to utilize spatial clustering methods to demarcate Local Climate Zones (LCZs) in Xi'an. Nevertheless, it became evident that the LCZ classification scheme employed was impracticable for subsequent urban planning and urban climate management. Therefore, we contend that a spatial index-based and supervised classification approach is more appropriate for the local climate zoning of Xi'an. Furthermore, a statistical analysis was conducted across 17 LCZ categories to affirm the rationality of the spatial classification. In adhering to the standardized data storage format as recommended by the LCZ system, this study has made a significant contribution to enriching the global database of urban morphologies within inland basins and high-density scenarios in China.

This research not only introduces an innovative approach to LCZ classification but also furnishes urban planners and policymakers with a valuable resource to inform their decisions pertaining to the sustainable development and management of Xi'an's urban environment. The adaptability of the improved LCZ system to the unique spatial characteristics of the city paves the way for more effective urban planning and control, thereby enhancing our comprehension of urban climatic conditions within the region. In the context of Xi'an's ongoing urbanization and development, the contributions of this study in terms of data integration and classification techniques can play a pivotal role in shaping a more resilient, comfortable, and sustainable urban landscape. However, it should be noted that this study does not delve into the potential socio-economic impacts of the LCZ classification. Future research endeavors can explore how these zoning strategies influence urban communities, their livelihoods, and overall well-being.

Author Contributions: Conceptualization, D.X. and D.Z.; Methodology, D.X., Q.Z. and Y.Y.; Software, D.X., Q.Z. and Y.Y.; Validation, D.X. and Q.Z.; Formal analysis, D.X., Q.Z. and Y.W.; Investigation, D.X. and Q.Z.; Resources, D.Z. and A.R.; Data curation, D.X., Q.Z. and Y.W.; Writing–original draft, D.X. and Q.Z.; Visualization, D.X. and Q.Z.; Supervision, A.R. All authors have read and agreed to the published version of the manuscript.

Funding: This research was funded by Shaanxi Province Natural Science Foundation, China, grant number 2022JQ-311 and China Postdoctoral Science Foundation funded project, grant number 2020M6834975.

Data Availability Statement: The data presented in this study are available on request from the corresponding author.

Conflicts of Interest: The authors declare no conflict of interest.

References

1. Lee, D.; Oh, K. Classifying urban climate zones (UCZs) based on statistical analyses. *Urban Clim.* **2018**, *24*, 503–516. [CrossRef]
2. Stewart, I.D.; Oke, T. Local Climate Zones for Urban Temperature Studies. *Bull. Am. Meteorol. Soc.* **2012**, *93*, 1879–1900. [CrossRef]
3. Guo, H.Z.Q.; Wang, J. Indicator System for Local Climate Zoning in Wuhan City: A Focus on Planning and Decision Making. Inheritance and Transformation. In Proceedings of the 2015 China Urban Planning Annual Conference, Guiyang, China, 19–21 September 2015; pp. 255–264.
4. Lelovics, E.; Unger, J.; Gál, T.; Gál, C.V. Design of an urban monitoring network based on Local Climate Zone mapping and temperature pattern modelling. *Clim. Res.* **2014**, *60*, 51–62. [CrossRef]
5. Alexander, P.J.; Mills, G. Local climate classification and Dublin's urban heat island. *Atmosphere* **2014**, *5*, 755–774. [CrossRef]
6. Leconte, F.; Bouyer, J.; Claverie, R.; Pétrissans, M. Using Local Climate Zone scheme for UHI assessment: Evaluation of the method using mobile measurements. *Build. Environ.* **2015**, *83*, 39–49. [CrossRef]
7. Zheng, Y.; Ren, C.; Xu, Y.; Wang, R.; Ho, J.; Lau, K.; Ng, E. GIS-based mapping of Local Climate Zone in the high-density city of Hong Kong. *Urban Clim.* **2018**, *24*, 419–448. [CrossRef]
8. Chen, F.H.Y. Construction of Local Climate Zoning Maps for Chengdu City Using the WUDAPT Method and Its Planning Applications. *Urban Archit.* **2018**, *20*, 29–32.
9. Cai, M.; Ren, C.; Xu, Y.; Lau, K.K.L.; Wang, R. Investigating the relationship between local climate zone and land surface temperature using an improved WUDAPT methodology—A case study of Yangtze River Delta, China. *Urban Clim.* **2018**, *24*, 485–502. [CrossRef]
10. Yang, X.; Yao, L.; Jin, T.; Peng, L.L.; Jiang, Z.; Hu, Z.; Ye, Y. Assessing the thermal behavior of different local climate zones in the Nanjing metropolis, China. *Build. Environ.* **2018**, *137*, 171–184. [CrossRef]
11. Yin, J.; Yin, Z.; Zhong, H.; Xu, S.; Hu, X.; Wang, J.; Wu, J. Monitoring urban expansion and land use/land cover changes of Shanghai metropolitan area during the transitional economy (1979–2009) in China. *Environ. Monit. Assess.* **2011**, *177*, 609–621. [CrossRef]
12. Patra, S.; Sahoo, S.; Mishra, P.; Mahapatra, S.C. Impacts of urbanization on land use /cover changes and its probable implications on local climate and groundwater level. *J. Urban Manag.* **2018**, *7*, 70–84. [CrossRef]
13. Das, M.; Das, A.; Mandal, S. Outdoor thermal comfort in different settings of a tropical planning region: A study on Sriniketan-Santiniketan Planning Area (SSPA), Eastern India. *Sustain. Cities Soc.* **2020**, *63*, 102433. [CrossRef]
14. Choudhury, D.; Das, A.; Das, M. Investigating thermal behavior pattern (TBP) of local climatic zones (LCZs): A study on industrial cities of Asansol-Durgapur development area (ADDA), eastern India. *Urban Clim.* **2021**, *35*, 100727. [CrossRef]
15. Singh, P.; Kikon, N.; Verma, P. Impact of land use change and urbanization on urban heat island in Lucknow city, Central India. A remote sensing based estimate. *Sustain. Cities Soc.* **2017**, *32*, 100–114. [CrossRef]

16. Murali, R.M.; Riyas, M.J.; Reshma, K.N.; Kumar, S.S. Climate change impact and vulnerability assessment of Mumbai city, India. *Nat. Hazards* **2020**, *102*, 575–589. [CrossRef]
17. Shi, Y.; Ren, C.; Luo, M.; Ching, J.; Li, X.; Bilal, M.; Fang, X.; Ren, Z. Utilizing world urban database and access portal tools (WUDAPT) and machine learning to facilitate spatial estimation of heatwave patterns. *Urban Clim.* **2021**, *36*, 100797. [CrossRef]
18. Ma, W.; Zeng, W.; Zhou, M.; Wang, L.; Rutherford, S.; Lin, H.; Liu, T.; Zhang, Y.; Xiao, J.; Zhang, Y.; et al. The short-term effect of heat waves on mortality and its modifiers in China: An analysis from 66 communities. *Environ. Int.* **2015**, *75*, 103–109. [CrossRef]
19. Mayrhuber, E.A.S.; Dückers, M.L.; Wallner, P.; Arnberger, A.; Allex, B.; Wiesböck, L.; Wanka, A.; Kolland, F.; Eder, R.; Hutter, H.P.; et al. Vulnerability to heatwaves and implications for public health interventions—A scoping review. *Environ. Res.* **2018**, *166*, 42–54. [CrossRef]
20. Wei, H.K.; Du, Z.P.Y.; Cui, H.; Yu, F. *China's Rural Development Report (2021) Agricultural and Rural Modernization towards 2035*; China Social Sciences Press: Beijing, China, 2021.
21. Das, M.; Das, A. Assessing the relationship between local climatic zones (LCZs) and land surface temperature (LST)—A case study of Sriniketan-Santiniketan Planning Area (SSPA), West Bengal, India. *Urban Clim.* **2020**, *32*, 100591. [CrossRef]
22. Kotharkar, R.; Bagade, A. Evaluating urban heat island in the critical local climate zones of an Indian city. *Landsc. Urban Plan.* **2018**, *169*, 92–104. [CrossRef]
23. Khamchiangta, D.; Dhakal, S. Future urban expansion and local climate zone changes in relation to land surface temperature: Case of Bangkok Metropolitan Administration, Thailand. *Urban Clim.* **2021**, *37*, 100835. [CrossRef]
24. Huang, K.; Leng, J.; Xu, Y.; Li, X.; Cai, M.; Wang, R.; Ren, C. Facilitating urban climate forecasts in rapidly urbanizing regions with land-use change modeling. *Urban Clim.* **2021**, *36*, 100806. [CrossRef]
25. Unal Cilek, M.; Cilek, A. Analyses of land surface temperature (LST) variability among local climate zones (LCZs) comparing Landsat-8 and ENVI-met model data. *Sustain. Cities Soc.* **2021**, *69*, 102877. [CrossRef]
26. Lau, K.K.-L.; Chung, S.C.; Ren, C. Outdoor thermal comfort in different urban settings of sub-tropical high-density cities: An approach of adopting local climate zone (LCZ) classification. *Build. Environ.* **2019**, *154*, 227–238. [CrossRef]
27. Geletič, J.; Lehnert, M.; Savić, S.; Milošević, D. Inter-/intra-zonal seasonal variability of the surface urban heat island based on local climate zones in three central European cities. *Build. Environ.* **2019**, *156*, 21–32. [CrossRef]
28. Hu, J.; Yang, Y.; Pan, X.; Zhu, Q.; Zhan, W.; Wang, Y.; Ma, W.; Su, W. Analysis of the Spatial and Temporal Variations of Land Surface Temperature Based on Local Climate Zones: A Case Study in Nanjing, China. *IEEE J. Sel. Top. Appl. Earth Obs. Remote Sens.* **2019**, *12*, 4213–4223. [CrossRef]
29. Geletič, J.; Lehnert, M.; Dobrovolný, P. Land Surface Temperature Differences within Local Climate Zones, Based on Two Central European Cities. *Remote Sens.* **2016**, *8*, 788. [CrossRef]
30. Collins, J.; Dronova, I. Urban Landscape Change Analysis Using Local Climate Zones and Object-Based Classification in the Salt Lake Metro Region, Utah, USA. *Remote Sens.* **2019**, *11*, 1615. [CrossRef]
31. Aslam, A.; Rana, I.A. The use of local climate zones in the urban environment: A systematic review of data sources, methods, and themes. *Urban Clim.* **2022**, *42*, 101120. [CrossRef]
32. Zhou, X.; Okaze, T.; Ren, C.; Cai, M.; Ishida, Y.; Mochida, A. Mapping local climate zones for a Japanese large city by an extended workflow of WUDAPT Level 0 method. *Urban Clim.* **2020**, *33*, 100660. [CrossRef]
33. János, U.; Enikő, L.; Mátyás, G.T. Local Climate Zone mapping using GIS methods in Szeged. *Földrajzi Értesítő* **2015**, *63*, 29–41.
34. Quan, S.J.; Bansal, P. A systematic review of GIS-based local climate zone mapping studies. *Build. Environ.* **2021**, *196*, 107791. [CrossRef]
35. Estacio, I.; Babaan, J.; Pecson, N.J.; Blanco, A.C.; Escoto, J.E.; Alcantara, C.K. GIS-based mapping of local climate zones using fuzzy logic and cellular automata. *Int. Arch. Photogramm. Remote Sens. Spat. Inf. Sci.* **2019**, *42*, 199–206. [CrossRef]
36. Hidalgo, J.; Dumas, G.; Masson, V.; Petit, G.; Bechtel, B.; Bocher, E.; Foley, M.; Schoetter, R.; Mills, G. Comparison between local climate zones maps derived from administrative datasets and satellite observations. *Urban Clim.* **2019**, *27*, 64–89. [CrossRef]
37. Kwok, Y.T.; Schoetter, R.; Lau, K.K.L.; Hidalgo, J.; Ren, C.; Pigeon, G.; Masson, V. How well does the local climate zone scheme discern the thermal environment of Toulouse (France)? An analysis using numerical simulation data. *Int. J. Climatol.* **2019**, *39*, 5292–5315. [CrossRef]
38. Zhan, Q.; Fan, Y.; Xiao, Y.; Ouyang, W.; Lan, Y.; Jin, Z.; Yin, J.; Zhang, L. Sustainable Strategy: Comprehensive Computational Approach for Wind Path Planning in Dense Urban Area. *Int. Rev. Spat. Plan. Sustain. Dev.* **2018**, *6*, 148–164. [CrossRef]
39. Wang, R.; Ren, C.; Xu, Y.; Lau, K.K.L.; Shi, Y. Mapping the local climate zones of urban areas by GIS-based and WUDAPT methods: A case study of Hong Kong. *Urban Clim.* **2018**, *24*, 567–576. [CrossRef]
40. Kaloustian, N.; Bechtel, B. Local Climatic Zoning and Urban Heat Island in Beirut. In Proceedings of the 4th International Conference on Countermeasures to Urban Heat Island (UHI), Singapore, 30 May–1 June 2016.
41. Cai, M.; Ren, C.; Xu, Y.; Dai, W.; Wang, X.M. Local Climate Zone Study for Sustainable Megacities Development by Using Improved WUDAPT Methodology—A Case Study in Guangzhou. In Proceedings of the International Conference on Geographies of Health and Living in Cities—Making Cities Healthy for All (H-Cities), Hong Kong, China, 21–24 June 2016.
42. Shi, Y.; Lau, K.K.L.; Ren, C.; Ng, E. Evaluating the local climate zone classification in high-density heterogeneous urban environment using mobile measurement. *Urban Clim.* **2018**, *25*, 167–186. [CrossRef]
43. He, S.; Zhang, Y.; Gu, Z.; Su, J. Local climate zone classification with different source data in Xi'an, China. *Indoor Built Environ.* **2019**, *28*, 1190–1199. [CrossRef]

44. Huang, F.; Jiang, S.; Zhan, W.; Bechtel, B.; Liu, Z.; Demuzere, M.; Huang, Y.; Xu, Y.; Ma, L.; Xia, W. Mapping local climate zones for cities: A large review. *Remote Sens. Environ.* **2023**, *292*, 113573. [CrossRef]
45. Perera, N.G.R.; Emmanuel, R. A "Local Climate Zone" based approach to urban planning in Colombo, Sri Lanka. *Urban Clim.* **2018**, *23*, 188–203. [CrossRef]
46. Xu, D. *Urban Spatial Planning to Cope with Urban Heat Island Effect*; China Architecture & Building Press: Beijing, China, 2022.
47. Han, B.; Luo, Z.; Liu, Y.; Zhang, T.; Yang, L. Using Local Climate Zones to investigate Spatio-temporal evolution of thermal environment at the urban regional level: A case study in Xi'an, China. *Sustain. Cities Soc.* **2022**, *76*, 103495. [CrossRef]

Disclaimer/Publisher's Note: The statements, opinions and data contained in all publications are solely those of the individual author(s) and contributor(s) and not of MDPI and/or the editor(s). MDPI and/or the editor(s) disclaim responsibility for any injury to people or property resulting from any ideas, methods, instructions or products referred to in the content.